

## Supplementary Materials for

### Evidence for a quantum spin Hall phase in graphene decorated with Bi<sub>2</sub>Te<sub>3</sub> nanoparticles

K. Hatsuda, H. Mine, T. Nakamura, J. Li, R. Wu, S. Katsumoto, J. Haruyama\*

\*Corresponding author. Email: j-haru@ee.aoyama.ac.jp

Published 9 November 2018, *Sci. Adv.* 4, eaau6915 (2018)

DOI: 10.1126/sciadv.aau6915

#### The PDF file includes:

Section S1. Formation of graphene to small Hall bar patterns with branches

Section S2. Nanoneedle decoration of Bi<sub>2</sub>Te<sub>3</sub> nanoparticles

Section S3. DFT calculation methods

Fig. S1. Designs of graphene Hall bars.

Fig. S2. DFT calculation results for Bi<sub>10</sub>Te<sub>15</sub>/graphene using an 8 × 8 supercell.

Fig. S3. Same as fig. S2, but for Bi<sub>11</sub>Te<sub>15</sub>/graphene in a 7 × 7 supercell.

Fig. S4. Spatial distributions of states at the tips of the Dirac cones for Bi<sub>10</sub>Te<sub>15</sub>/graphene in a 7 × 7 supercell.

Legend for movie S1

References (32–38)

#### Other Supplementary Material for this manuscript includes the following:

(available at [advances.sciencemag.org/cgi/content/full/4/11/eaau6915/DC1](https://advances.sciencemag.org/cgi/content/full/4/11/eaau6915/DC1))

Movie S1 (.MOV format). How to decorate Bi<sub>2</sub>Te<sub>3</sub> nanoparticles with very low amount by a nanoneedle.

### Section S1. Formation of graphene to small Hall bar patterns with branches

CVD-grown monolayer graphene with  $1\text{cm}^2$  area is formed into nine segments (fig. S1A), including the two Hall-bar patterns with six or four branches in individual segments, by Ar gas etching (Fig. 1D in the main text and figs. S1B and S1C). Before performing this etching, a resist mask is patterned by electron beam. Because the areas of the Hall-bar patterns are very small, this resist mask for Hall-bar patterns is detached from the graphene surface after electron-beam irradiation and developing the resist. To avoid this trouble (i.e., disappearance of the resist masks for graphene etching), triangle patterns with a large area are attached to ends of the six or four branches of the Hall bar patterns as shown in fig. S1C. These triangular graphene areas are finally covered by metal electrodes, and so do not influence the present experiments.

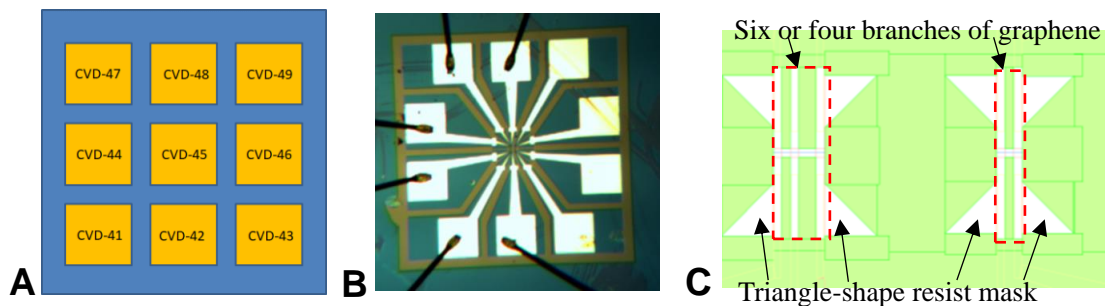


**Fig. S1. Designs of graphene Hall bars.** (A) Schematic view of nine segments formed on CVD-grown monolayer graphene. (B) Optical microscope view of one segment of (A) with wire bonding on electrode pads. (C) Schematic view of two Hall-bar patterns with six or four branches in the center part of (B).

## **Section S2. Nanoneedle decoration of Bi<sub>2</sub>Te<sub>3</sub> nanoparticles**

There exist many methods to decorate graphene (or other material surface) by nanoparticles, which result in various phenomena and applications. Some methods (e.g., sputtering and evaporation) lead to undesired chemical effects and parasitic phenomena due to damage and contamination, such as intervalley scattering, spin absorption, and diffusive charge transport. The present nanoneedle method directly places nanoparticles on graphene and can minimize such parasitic effects.

Before the Bi<sub>2</sub>Te<sub>3</sub> nanoparticle decoration, an acetone solution containing the nanoparticles (Sigma Aldrich Inc.) is ultrasonicated for 3-5 hours by low power to obtain much smaller particle diameters (e.g., < 1nm) by crushing them, avoiding introduction of defects to nanoparticles. Then, low amount of acetone solution containing Bi<sub>2</sub>Te<sub>3</sub> nanoparticles (e.g., 0.01mg/8ml) is dropped from the top end of the nanoneedle (Saito Medical Instruments Inc.) on the two neighboring Hall-bar patterns of graphene (fig. S1C). This droplet on graphene is then absorbed by the nanoneedle (see accompanying video). We repeat this dropping and absorbing 10-20 times, resulting in the controlled decoration of Bi<sub>2</sub>Te<sub>3</sub> nanoparticles with very low density (< 5% coverage).

The obtained density and distribution of nanoparticles on the patterned graphene is sensitive to the density of nanoparticles contained in acetone solution, time for ultrasonication of the solution, position to absorb the solution by a nanoneedle from a container right after the ultrasonication, and the number of times to repeat the dropping and absorbing as mentioned above. Thus, careful optimization is required. Because the deposited nanoparticles are spread over a large area of the sample (e.g., over the region for fig. S1B) depending on this optimized

condition, a passivation film with an open window only on graphene surface (*e.g.*, fig. S1C) is needed. After the decoration, each sample is annealed at 400 °C for 10-15 minutes under a high vacuum ( $10^{-6}$  Torr) for surface cleaning. These annealing conditions are the upper limit to keep quality of the nanoparticles. Indeed, nanoparticles annealed at 450 °C with the same time and vacuum degraded.

### **Section S3. DFT calculation methods**

Our DFT calculations were carried out by Vienna ab-initio simulation package (VASP) [32-33] at the level of the generalized-gradient approximation (GGA) with the parameterized exchange-correlation functional developed by Perdew-Burke- Ernzerhof (PBE) [34]. We treated C-2s2p, Te-5s5p and Bi-6s6p as valence states and describe the interaction between valence electrons and ionic cores within the framework of the projector augmented wave (PAW) method [35-36]. For the structural relaxation, the non-local van der Waals density functional was used [37-38], and all atoms were fully relaxed using the conjugated gradient method for the energy minimization until the force on each atom became smaller than  $0.01\text{eV}/\text{\AA}$ . The energy cutoff for the plane wave expansion was set to 700eV, which is sufficient for the system according to our test calculations.

Figures S2 and S3 show DFT results for different configurations of nanoparticles on graphene, illustrating the variability of the induced topological band gap. Figure S4 shows the intermixing of graphene, Bi, and Te orbitals for states across the gap.

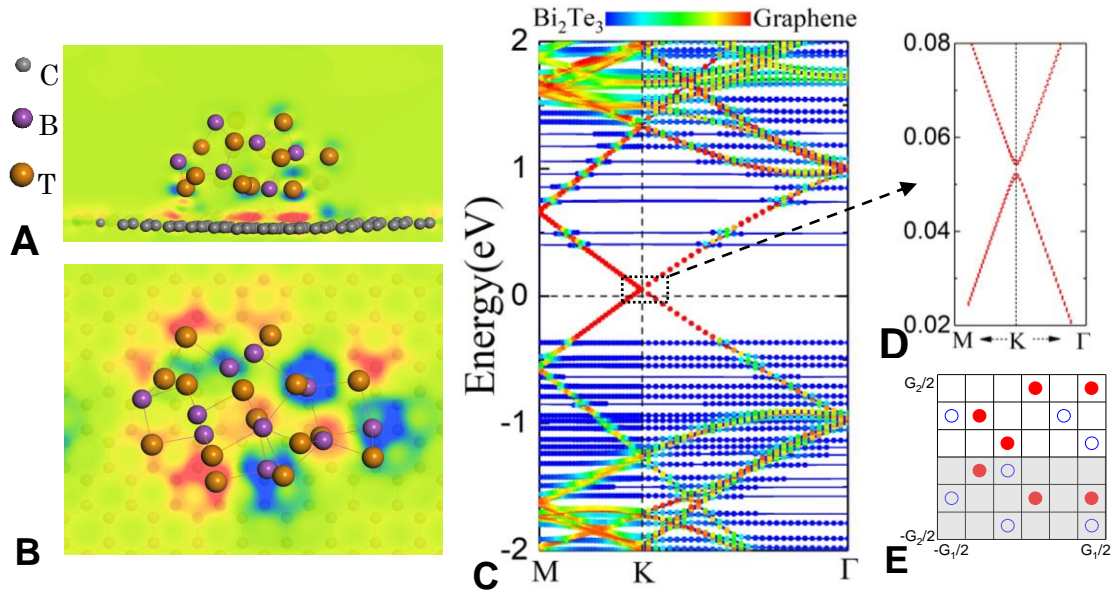


**Fig. S2. DFT calculation results for Bi<sub>10</sub>Te<sub>15</sub>/graphene using an 8 × 8 supercell.** (A) Side and (B) top views of the charge-density difference of Bi<sub>10</sub>Te<sub>15</sub>/Graphene using an 8×8 supercell. Red and blue colors indicate charge depletion and accumulation. (C,D) Band structure of Bi<sub>2</sub>Te<sub>3</sub>/Graphene (8×8) with SOC; the band gap is about 3meV. (E) Corresponding n-field configuration. The red solid and blue hollow circles denote n= -1 and n= 1, respectively, while blank entries denote n= 0. Summing the n-field over half of the torus yields a nontrivial Z<sub>2</sub> invariant.

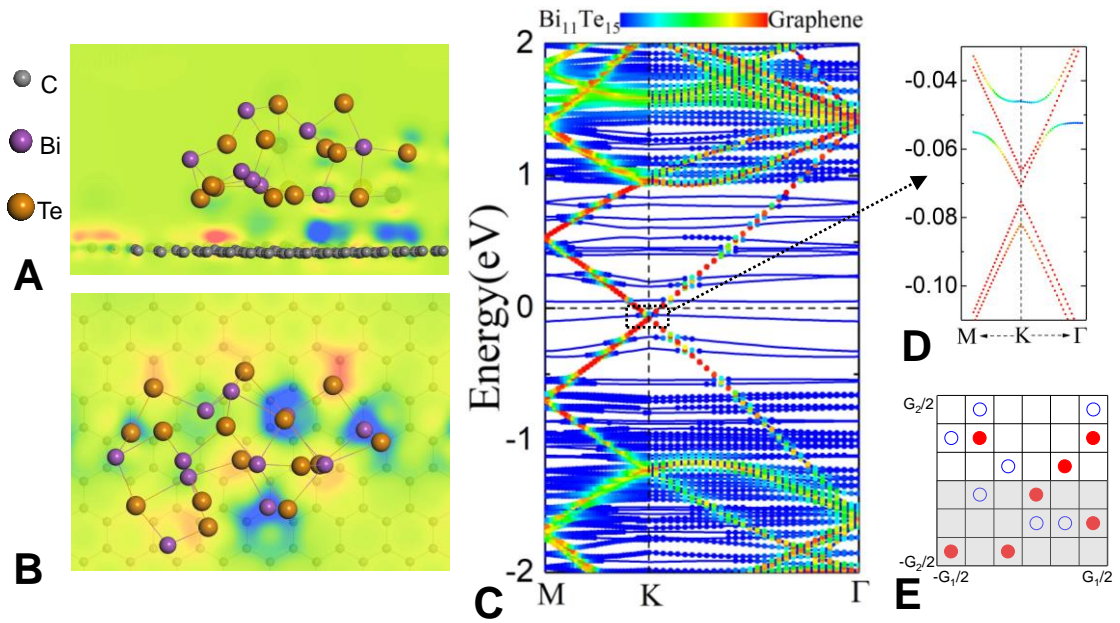


**Fig. S3.** Same as fig. S2, but for  $\text{Bi}_{11}\text{Te}_{15}$ /graphene in a  $7 \times 7$  supercell. Here the band gap is about 5.6 meV, and the  $Z_2$  invariant is again nontrivial.

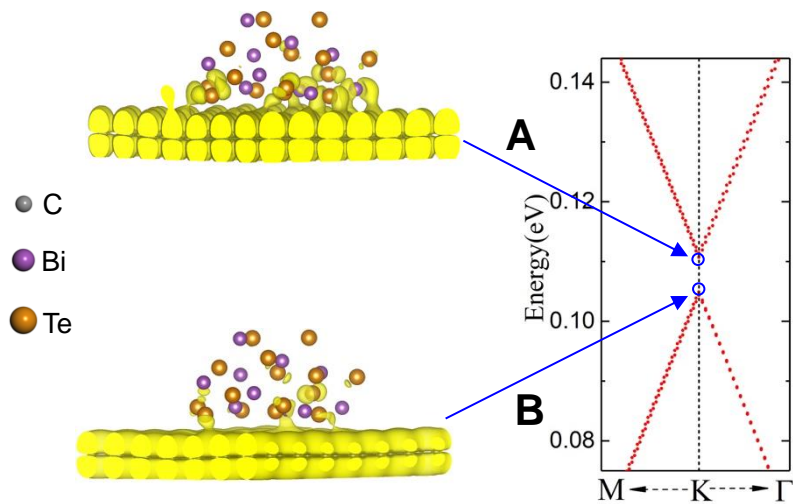


**Fig. S4.** Spatial distributions of states at the tips of the Dirac cones for  $\text{Bi}_{10}\text{Te}_{15}$ /graphene in a  $7 \times 7$  supercell.

**Movie S1. How to decorate Bi<sub>2</sub>Te<sub>3</sub> nanoparticles with very low amount by a nanoneedle.** The present nanoneedle method directly places nanoparticles on graphene and minimizes parasitic effects. Low amount of acetone solution containing Bi<sub>2</sub>Te<sub>3</sub> nanoparticles is dropped from the top end of the nanoneedle on the Hall-bar patterns of graphene. This droplet on graphene is then absorbed by the nanoneedle. The dropping and absorbing are repeated in 10-20 times. This results in the controlled decoration of Bi<sub>2</sub>Te<sub>3</sub> nanoparticles with very low density (< 5% coverage).